

# Dynamic Model and Optimal Control of a Fully Parallel Manipulator

Victor Renan Bolzon<sup>1</sup>, Thamiris Lima Costa<sup>2</sup>, Edson Hideki Koroishi<sup>3</sup>, Fabian Andres Lara-Molina<sup>4</sup>

Department of Mechanical Engineering,  
Federal University of Technology - Paraná  
Cornélio Procópio, Paraná, Brazil

**Abstract**— The purpose of this paper is to analyze the dynamics and also to project the optimal control system of the full six parallel manipulator Stewart-Gough Platform. Based on the full dynamic model and simulations, the position control is design based on the Linear Quadratic Regulator (LQR) and the Computed Torque Control (CTC) techniques, these techniques are applied in order to reduce the trajectory tracking error at the workspace. Also a Proportional Derivative Controller (PD) together with the CTC technique was set to evaluate the trajectory tracking performance of the LQR controller.

**Keywords**—Dynamic Modeling; Position Control; Linear Quadratic Regulator, Computed Torque Control;

## I. INTRODUCTION

Recently, the parallel robots have been widely applied in several fields of the engineering, as for example: flight simulators, industrial machines and due its high precision of movements, they have also been applied as surgical robots [1]. For this aims, it is necessary to improve the performance of these manipulators, to increase the stability and efficiency, although with low operational costs. For this reason, many researches have been realized in this field. As [2], that proposed through two proposed parameters, with the genetic algorithm to optimize the dynamic project of a parallel manipulator. [3] presented a controller based on the adaptive law, where the constant feedback gains of the PD controller was substituted into other no-linear time variables.

Reference [4] implemented the direct dynamic of the Stewart-Gough manipulator by using Matlab<sup>®</sup>, based on the Kane equation, where the forces for each actuator and the initial conditions are given, so its obtained the position and orientation of the manipulator and for the actuators are found the linear velocity and the position. [5] used a cascade control system to track the trajectory of 6-DOF parallel robot. It was considered not only the mechanical dynamic, but also the dynamics of hydraulic actuators.

Fuzzy control was used by [6] for the set-point regulation of a two-link planar robot with flexible joints. This set-point regulation control is applied to find a feedback control law to reduce the vibration on the joints. [7] used a Neuro-fuzzy adaptive control in a Stewart-Gough manipulator with rotary actuators, each revolute link was trained under different loadings and maneuvers. So, they learned how to collaborate with the others to complete a task, for example, a desired trajectory.

Reference [8] made a review of Stewart-Gough manipulator control schemes, in order to obtain a high performance control strategy design. Based on some analysis

of the systems a Incremental Nonlinear Dynamic Inversion controller is used to deal with the hydraulic actuator. Recently, [9] proposed a self-calibration method to improve the accuracy performance of a 6-DOF parallel manipulator. The numerical simulations of this paper showed a considerable reduction on the parameters errors as in the position and orientation accuracy of the manipulator.

On an Orthoglide robot, [10] used a generalized predictive control technique (GPC) to check the benefits of the strategy on the dynamic performance of the robot in terms of accuracy, disturbance rejection. This strategy, is composed of two control loops. The inner loop linearize the nonlinear dynamics using feedback linearization. And the outer loop tracks the desired trajectory based on the GPC method.

The dynamic model of a parallel manipulator allows implementing the computational simulation, where the main characteristics from the kinematics and dynamics movement can be known and studied. Based on the dynamic simulation of the robot, it is possible to project the motion control system. As an additional benefit, the computer simulations decrease the project costs, because they permit to know previously the dynamic behavior, singularities and potential errors of the manipulator project before its construction.

The purpose of this paper is to analyze the dynamic response and to project the position control system of the Stewart-Gough manipulator. Initially, in order to analyze the complete dynamics and computational simulations of the manipulator, step forces are applied on the actuators to simulate the dynamic response. Then, the position control system is design based on the LQR and CTC control techniques.

The remain of this paper is organized as follows. Section II presents the Stewart-Gough manipulator model. The LQR and CTC methods are presented in Section III. Section IV gives the numerical results. Finally, some conclusion and further work are enumerated.

## II. STEWART-GOUGH MANIPULATOR MODEL

The parallel manipulator used in this contribution is the Stewart-Gough platform, as can be seen at the Fig. 1, has six identical legs, that connects a fixed base to a movable platform by passive universal joints represented by  $U$  on the points  $B_i$ , at the points  $A_i$  are the passive spherical joints, defined as  $A_i$ , where  $i = 1, \dots, 6$ , subsequently. The legs are divided in an upper and a lower member by Prismatic joints, showed at Fig. 1 as  $P$ . The Prismatic joint has a motor that extend and retract the leg. The movable platform has six degrees of freedom (DOF), which are three angular motions expressed as Euler

angles with respect to  $x$ - $y$ - $z$ -axes and three longitudinal linear motions at the  $x$ - $y$ - $z$  axes. According to the paper developed by [11], will be demonstrated, based on the Newton-Euler approach, the model kinematic and dynamic model of the Stewart-Gough Platform.

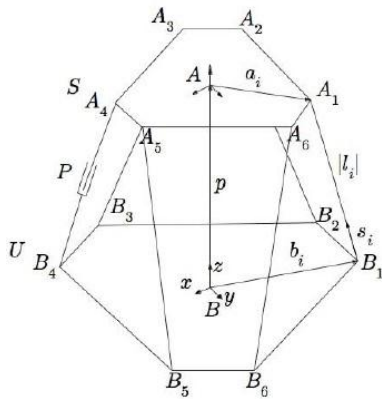


Fig. 1. Stewart-Gough Manipulator.

A. Legs Kinematics and Dynamics

The inverse kinematics represent the six legs length  $l_i = [l_1, \dots, l_6]^T$  as function of the position  $p$  and orientation of the Euler angles  $\theta$  of the movable platform. So,  $p = [x \ y \ z]^T$  and  $\theta = [\alpha \ \beta \ \gamma]^T$  results in a rotational matrix  $R = R_x(\alpha)R_y(\beta)R_z(\gamma)$ . In this way, considering the close vector chain  $\{B\}\{A\}A_iB_i$ . Thus, the inverse kinematic model for each leg is:

$$l_i = Ra_i + p + b_i \quad L_i = ||l_i|| \quad (1)$$

The unit vector along  $l_i$  is  $s_i = l_i/L_i$ . The velocity at the point  $A_i$  from the movable platform is:

$$\dot{l}_i = \omega \times a_i + \dot{p} \quad (2)$$

where  $\omega$  is the angular velocity of the movable platform. The relative velocity between the upper and the lower member of the legs  $\dot{l}_i = s_i \cdot \dot{l}_i$ ; similarly, the angular velocity of the legs is  $\omega_{bi} = s_i \times l_i/L_i$ . Consequently, the acceleration at points  $A_i$  of the movable platform is:

$$\ddot{l}_i = \underbrace{\ddot{p} + \alpha + a_i}_{a_p} + \underbrace{\omega \times (\omega \times a_i)}_{h_1} \quad (3)$$

The acceleration of the center of gravity lower and upper parts of the legs are respectively:

$$a_{di} = \frac{1}{L_i}(s \times a_p) \times r_{di} + h_{3i}$$

$$a_{ui} = (s_i \cdot a_p) \cdot s_i + \frac{1}{L_i}(s_i \times a_p) \times r_{ui} + h_{4i} \quad (4)$$

where  $r_{di}$  and  $r_{ui}$  are the centers of gravity of lower and upper part,  $= h_{2i} \times r_{di} + \omega(\omega \times r_{di})$  and  $h_{4i} = us_i + h_2 \times r_{ui} + \omega \times (\omega \times r_{ui}) + 2\dot{l}\omega$ ,  $h_{2i} = \frac{1}{L_i}(s_i \times h_1 - 2l_i\omega)$ . Considering

the dynamic analysis, the Euler equation is applied for the rotational equilibrium of the entire leg, thus:

$$m_{di} \cdot r_{di} \times a_{di} - m_{ui} \cdot r_{ui} \times a_{ui} + (m_{di} \cdot r_{di} + m_{ui} \cdot r_{ui}) \times g - (I_{di} + I_{ui}) \cdot \Lambda_{bi} - \omega_b \times (I_d + I_u) \cdot \omega_{bf} + M_{ui} \cdot s_i + l_i \times f_{si} - c_{ui} \omega_{bi} - f_i = 0 \quad (5)$$

$\Lambda_{bi}$  is the acceleration of the leg,  $f_{si}$  is the constraint force at the spherical joint acting on the leg,  $f_i$  represents the moment of viscous friction at the  $i$ -th spherical joint  $f_i = c_{st}(\omega_{bt} - \omega_t)$  and  $f_{li}$  is the input force at the  $i$ -th leg. For the upper part of the leg, the translational equilibrium is:

$$f_{li} + s_i \cdot f_{si} - c_{pi} \cdot \dot{l}_i - m_{ui} \cdot s_i \cdot g = 0 \quad (6)$$

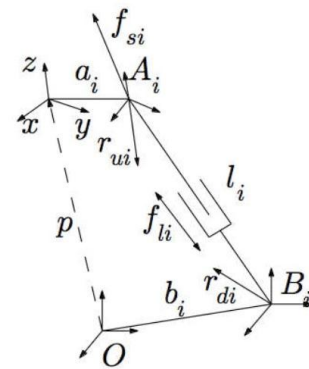


Fig. 2. Leg of the Stewart-Gough Manipulator.

The equation that expresses,  $f_{si}$  results of some substitution between equations above, it has a lot of terms almost all depends on the constraint force at the spherical joint acting on the leg, results substitution between the equations presented before, where many terms are dependent of  $a_p$ . Thus, in order to use this expression in the dynamic equations of the platform, all these terms are grouped in the form (Q, a  $3 \times 3$  matrix), thus:

$$f_{si} = Qa_p + v - s_i \cdot f_{li} \quad (7)$$

Where,

$$Q = \left[ m_{ui} \cdot \left( 1 + \frac{2s_i \cdot r_{ui}}{L_i} \right) - \frac{m_{di} \cdot r_{di}^2 + m_{ui} \cdot r_{ui}^2}{L_i^2} \right] \cdot s_i \cdot s_i^T + \frac{m_{di} \cdot r_{di}^2 + m_{ui} \cdot r_{ui}^2}{L_i^2} \cdot - \frac{m_{ui}}{L_i} (s_i \cdot r_{ui}^T + r_{ui} \cdot s_i^T) - \frac{1}{L_i^2} [m_{di} \cdot (s_i \times r_{di}) \cdot (s_i \times r_{ui})^T + m_{ui} \cdot (s_i \times r_{ui}) \cdot (s_i \times r_{ui})^T - \tilde{s}_i \cdot (I_d - I_u) \tilde{s}_i]$$

Finally, after some substitution of  $a_p$  by its expression in (3), this equation represents the reaction force of the  $i$ -th (see Fig.2) point of connection of the platform:

$$f_{si} = Q_i \cdot \ddot{p} - Q_i \cdot a_i \cdot \alpha + v_i - s_i \cdot f_{li} \quad (8)$$

B. Dynamics and kinematics of the movable platform

By applying the expression of (8) for the six legs ( $i = 1, \dots, 6$ ), the dynamic equations of the platform can be formulated. The acceleration of the center of gravity of the platform respect to the reference frame is:

$$a_p = \alpha \times r_{pA} + \omega \times (\omega \times r_{pA}) + \ddot{p} \quad (9)$$

where,  $r_p = Rr_{pA}$  and  $r_{pA}$  expresses the distance of the center of gravity of the platform to the frame  $\{A\}$ .

Applying the Newton equation for translational equilibrium and the Euler equation for rotational equilibrium of the platform, we have respectively:

$$m_p \cdot a_p + m_p \cdot g - \sum_{i=1}^6 (f_{si}) = 0 \quad (10)$$

$$m_p \cdot r_{pA} \times a + m_p \cdot r_{pA} \times g - I \cdot \alpha - \omega \times I_p \cdot \omega + \sum_{i=1}^6 [a_i \times f_{si}] + \sum_{i=1}^6 f_i = 0 \quad (11)$$

$m_p$  represents the mass and  $I_p = RI_{pA}R^T$  the inertia of platform and payload. Finally, the expressions of  $a_p$  and  $f_{si}$  are substituted into the Newton equations and Euler equations and the complete dynamic of the platform is obtained:

$$J \cdot \begin{bmatrix} \ddot{p} \\ \alpha \end{bmatrix} + \eta = H \cdot f_l \quad (12)$$

where,  $J = J_p + \sum_{i=1}^6 J_i$ ;  $\eta = \eta_p + \sum_{i=1}^6 \eta_i$  e  $J_p = \begin{bmatrix} m_p \cdot I & -m_p \cdot \tilde{r}_p \\ m_p \cdot \tilde{R} & I_p + m_p (\|r_p\|^2 \cdot I - r_p \cdot r_p^T) \end{bmatrix}$ ,  $J_i = \begin{bmatrix} Q_i & -Q_i \\ \tilde{a}_i \cdot Q_i & -\tilde{a}_i \cdot Q_i \cdot \tilde{a}_i \end{bmatrix}$ ,  $\eta_p = \begin{bmatrix} m_p \cdot [\omega \times (\omega \times r_p) - g] \\ \omega \times I_p \cdot \omega + m_p R \times [(\omega \cdot r_p) \cdot \omega - g] \end{bmatrix}$ ,  $\eta_i = \begin{bmatrix} V_i \\ a_i \times V_i - f_{li} \end{bmatrix}$ ,  $H = \begin{pmatrix} s_1 & \dots & s_6 \\ a_1 \times s_1 & \dots & a_6 \times s_6 \end{pmatrix}$ , this matrix describes the Jacobian matrix of the manipulator, and  $f_{li} = [f_{li} \dots f_{i6}]^T$ . The joint-space dynamic equations are obtained with using the sliding acceleration of a prismatic joint of the  $i$ -th leg:

$$\begin{bmatrix} \ddot{p} \\ \alpha \end{bmatrix} = H^T (\ddot{L}_i - u) \quad (13)$$

Finally, it is obtained the dynamic equation of the Stewart-Gough robot in joint space is:

$$H^{-1} J H^{-T} \ddot{L}_i + H^{-1} (\eta - J H^{-T} u) = f_l \quad (14)$$

### III. CONTROL SYSTEM

#### A. Computed Torque Control

It is necessary to apply the CTC method, linearize the non-linear dynamic (14). As  $A(L) = H^{-1} J H^{-T}$  and  $B(L, \dot{L}) = H^{-1} (\eta - J H^{-T} u)$ , the dynamic non-linear equation of the manipulator can be represented as:

$$f_l = A(L) \ddot{L} + B(L, \dot{L}) \quad (15)$$

Thus, the manipulator dynamic equation is linearized and decoupled by nonlinear feedback. So,  $\hat{A}(L)$  and  $\hat{B}(L, \dot{L})$  can be estimated as  $A(L)$  and  $B(L, \dot{L})$ . Considering that  $\hat{A}(L) = A(L)$  and  $\hat{B}(L, \dot{L}) = B(L, \dot{L})$ , so is reduced to a linear control on decoupled double-integrators, where:

$$\ddot{q} = w \quad (16)$$

So  $w$  is the new input control vector. Where this equation represents the inverse dynamic control scheme, which the dynamic direct model is turned into a double set of integrators. In this way, the control method can be used to project the tracking position control. Assuming that the requested trajectory is described with the desire position  $L^d$ , velocity  $\dot{L}^d$  and the acceleration  $\ddot{L}^d$ . So, the control law for the PD controller is:

$$w = L^d + K_P (L^d - L) + K_D \frac{d}{dt} (L^d - L) \quad (17)$$

Where  $K_P = \text{diag}(k_{p1}, \dots, k_{p6})$  and  $K_D = \text{diag}(k_{d1}, \dots, k_{d6})$  are the controller gain matrices.

The gain of the controller are obtained to have the closed-loop characteristic equation of the controlled system:  $(s^2 + 2\varepsilon\omega_r s + \omega_r^2) = 0$ ,  $s$  represents the Laplace variable. Thus,  $k_P = \omega_r^2$ ,  $k_D = \varepsilon\omega_r$ .

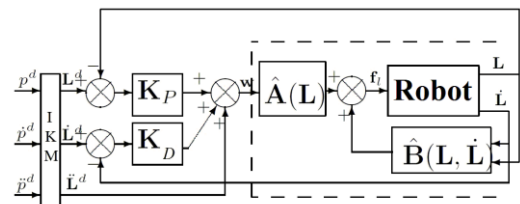


Fig. 3. CTC and PD Control

#### B. Linear Quadratic Regulator

The quadratic optimal control method is a systematic form to determinate the feedback control gain of the state matrix form. In the LQR controller project, is considered a time invariant, which is given by the state space system representation:

$$\dot{x}(t) = Ax(t) + Bu(t) \quad (18)$$

$$y(t) = Cx(t) + Du(t) \quad (19)$$

where  $A$ ,  $B$ ,  $C$  and  $D$  represent the state matrices,  $x(t)$  is the model state vector,  $u(t)$  is input vector,  $y(t)$  is the generic system output. [6]. Thus, the state feedback is defined as:

$$u(t) = -Kx(t) \quad (20)$$

$K$  is the state feedback matrix. Substituting (20) into (18), it is obtained the closed-loop response:

$$\dot{x}(t) = (A - BK)x(t) \quad (21)$$

To obtain the optimal gain, the following equation must be minimized:

$$J = \int_0^\infty [x(t)^T Q x(t) + u(t)^T R u(t)] dt \quad (22)$$

Where the matrices Q and R are responsible for the error and the energy consumption. With Q and R, the feedback matrix is represented by:

$$K = R^{-1}B^T P, \tag{23}$$

which  $P = P^T \geq 0$  must satisfied the Riccati algebraic equation. [6].

$$A^T P + PA - PBR^{-1}B^T + Q = 0 \tag{25}$$

#### IV. RESULTS

In order to study the dynamic response by the influence of the actuators action, six pulse generators applied a 1N force during 0.5 seconds at each leg of the Stewart-Gough manipulator, which was at a determined initial position. This is important to understand the dynamic characteristics of the manipulator and to project the controller.

For the control simulations, both controller were tuned using the methods presented at section III. To analyze the performance of the techniques, two simulations were realized. First, a simulation to evaluate the tracking position for a determined circular trajectory. The second simulation was about the reaction of the controllers, when the manipulator at fixed initial position suffer a perturbation and had to return to the initial position. The parameters used in the simulations (see Tab. I), were obtained at [12].

##### A. Dynamic Analysis

To the dynamic analysis was implemented in a computational simulation, through the Matlab/Simulink® software. A simulation, where six pulse generators applied a force, to imitate the action from the actuators, which is applied a 1N force for 0.5 seconds in each leg of the Stewart-Gough manipulator. At the Fig. 4, it is possible to see, the initial position of the mechanism and after the application of the force, the final position.

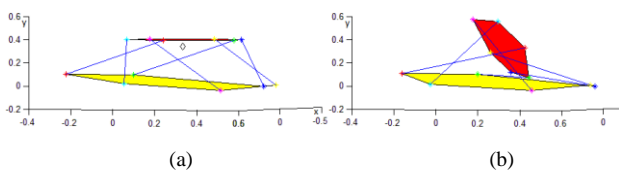


Fig. 4. Initial and Final position of the Stewart Platform.

It is showed at the Fig. 5, the initial positions of the legs and the displacement of the legs during the actuators force application. The Fig. 6 shows the velocity of the six legs of the manipulator from the repose and during the application of the force, in a pulse form, during 0.5 seconds. With these results, is possible to see the reaction of the legs of the Stewart-Gough manipulator, during the application of the forces from the actuators.

##### B. Control

The control methods previous presented, were used to determinate the gain of the controllers. To the computational simulation was used again the parameters of [1] and the dynamic equation presented previously.

TABLE I.

Dynamic Parameters for Simulation	
Parameter	Value
$a_i$	$\begin{bmatrix} 0.3 & 0.0 & 0.1 \\ 0.3 & 0.2 & 0.0 \\ 0.0 & 0.3 & 0.0 \\ -0.2 & 0.1 & -0.1 \\ -0.15 & -0.2 & -0.05 \\ 0.15 & -0.15 & -0.05 \end{bmatrix} m$
$b_i$	$\begin{bmatrix} 0.6 & 0.2 & 0.0 \\ 0.1 & 0.5 & 0.1 \\ -0.3 & 0.3 & 0.1 \\ 0.3 & -0.4 & 0.0 \\ 0.2 & -0.3 & -0.05 \\ 0.5 & -0.2 & 0.0 \end{bmatrix} m$
$m_p$	40 kg
$m_d$	3 kg
$m_u$	1 kg
$r_d$	$[0.4 \ 0.14 \ -0.18]^T m$
$r_u$	$[-6 \ 0.08 \ -0.08]^T m$
$r_p$	$[0.04 \ 0.03 \ -0.06]^T m$
$I_d$	$\begin{bmatrix} 0.010 & 0.005 & 0.007 \\ 0.005 & 0.002 & 0.003 \\ 0.007 & 0.003 & 0.001 \end{bmatrix} Kg.m^2$
$I_u$	$\begin{bmatrix} 0.005 & 0.002 & 0.002 \\ 0.002 & 0.002 & 0.001 \\ 0.002 & 0.001 & 0.003 \end{bmatrix} Kg.m^2$
$I_p$	$\begin{bmatrix} 0.05 & 0.003 & 0.004 \\ 0.003 & 0.004 & 0.003 \\ 0.004 & 0.003 & 0.100 \end{bmatrix} Kg.m^2$

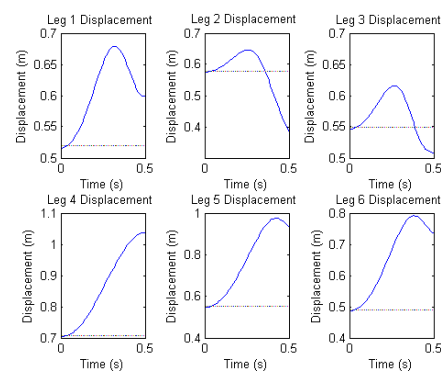


Fig. 5. Legs Displacement.

The PD controller was tuned to obtain a stable response without overshoot,  $\omega_r = 35 \text{ rad/s}$  e  $\xi = 1$ . Thus, the gains was obtained with the equations presented at the chapter III,  $k_P = [1225 \ 1225 \ 1225 \ 1225 \ 1225 \ 1225]^T$  and  $k_D = [35 \ 35 \ 35 \ 35 \ 35 \ 35]^T$ .

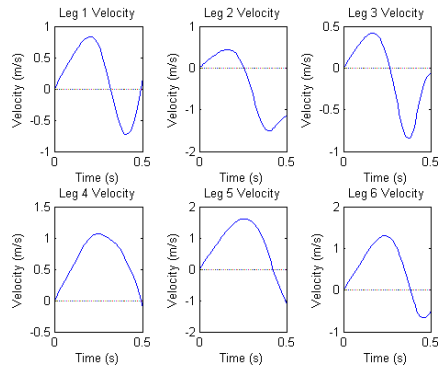
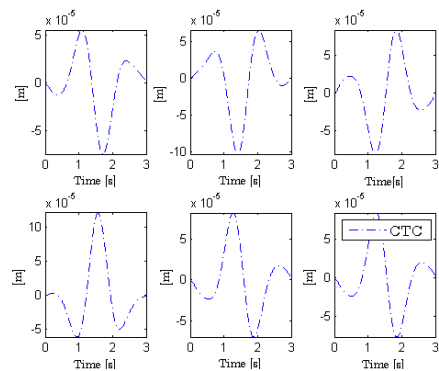
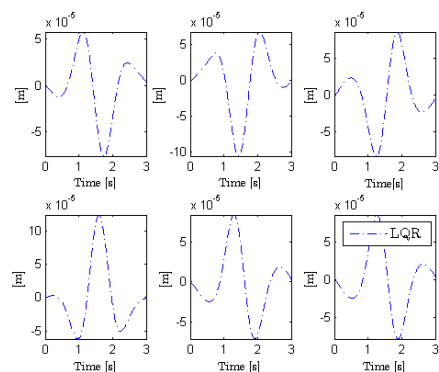


Fig. 6. Legs Displacement.

The LQR was tuned to satisfy similar characteristics of the PD. Based on the linearized model for each joint of the Eq. 16, the system matrices of the Eq. 18 and Eq.19, was defined as:  $A = \begin{bmatrix} 0 & 1 \\ 0 & 0 \end{bmatrix}$ ,  $B = [0 \ 1]^T$ ,  $C = [1 \ 0]$  e  $D = [0]$ . To define the LQR control matrices, the values of  $Q$  and  $R$ , were obtained after simulations as  $Q = \begin{bmatrix} 160000 & 0 \\ 0 & 253 \end{bmatrix}$  and  $R = [0,1]$ . Consequently, we get the gain of the controller  $k_P = [1264 \ 1264 \ 1264 \ 1264 \ 1264 \ 1264]^T$  and  $k_D = [71 \ 71 \ 71 \ 71 \ 71 \ 71]^T$ . In the next figure, it is possible to see the circular trajectory of the movable platform at the workspace, which is used to evaluate the controllers:



(a)



(b)

Fig. 8. Tracking error of the joints.

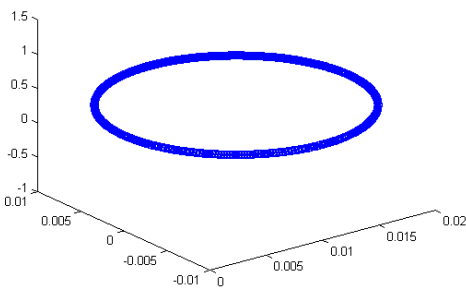


Fig. 7. Tracking trajectory.

The Fig 8. shows the error in the tracking of the joints for the PD and the LQR methods, respectively. It can be observed that both controllers have a similar result. At the Fig 9. and Fig 10. are presented the behavior of the forces of the six actuators through the control methods PD and LQR, for the trajectory showed on the Fig.7. On both cases, the results are equivalent, because of the gains obtained for these methods are similar.

The last test simulation shows the disturbance reaction, when the movable platform is in a fixed initial position  $p = [0 \ 0 \ 0,395m \ 0 \ 0 \ 0]^T$  and is applied a 5N step force at  $z$ -axis. How it can be seen, at Fig. 11, for the both controls techniques, which the Fig. 11(a) on represents the PD and Fig. 11(b) is the LQR. Comparing the PD with the LQR result, it is possible to see a light attenuation on the overshooting during the stabilization, because the LQR method has a better damping compared with the PD method.

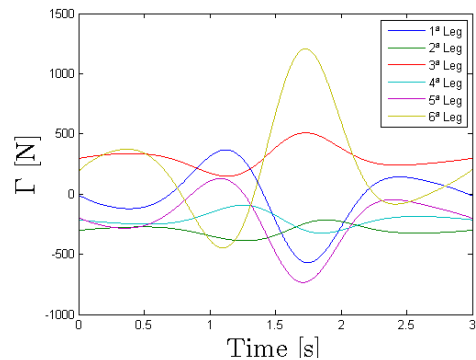


Fig. 9. Force control for the six atuators using CTC method.

## V. CONCLUSION

First, in this contribution was presented the Stewart-Gough manipulator model, where the kinematic and dynamics equations were showed. After this, was introduced the controller methods used to tune the controller on this paper. With the model was possible to do some numerical simulations and also project the of the controllers.

The dynamic simulations showed how the behavior of the Stewart-Gough manipulator during the force application, in a pulse form, in each leg of the manipulator. This was fundamental to project the controller. The results of the

controller simulations were similar, but it is important the optimal tuned way with the LQR method.

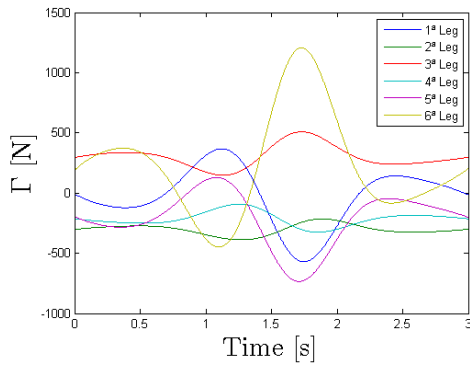
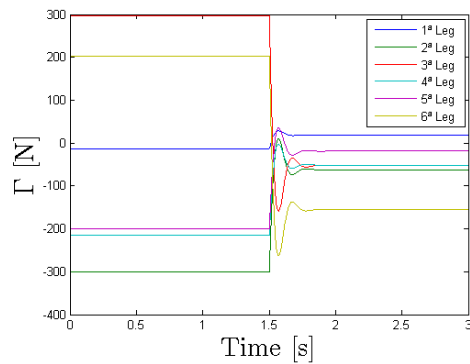
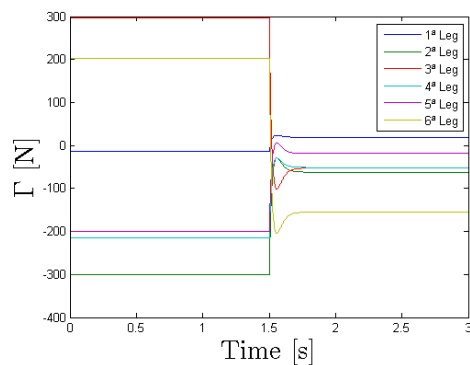


Fig. 10. Force control for the six actuators using CTC method.



(a)



(b)

Fig. 11. Disturbance reaction for both methods.

### ACKNOWLEDGMENT

The authors express their acknowledgements to the Graduate Program of Mechanical Engineering, jointly funded by CAPES.

### REFERENCES

- [1] M. Wapler, V. Urban, T. Weisener, J. Stallkamp, M. Durr, and A. Hiller, "A Stewart platform for precision surgery," *Transactions of the Institute of Measurement and Control*, vol. 25, no. 4, pp. 329-334, 2003.
- [2] J. Kilaru, M.K. Karnam, S. Agarwal and S. Bandyopadhyay, "Optimal design of parallel manipulators based on their dynamic performance," In *Proceedings of the 14th IFToMM World Congress*, 2015, pp. 406-412.
- [3] Bennehar, M., Chemori, A.; Pierrot, F. A new revised desired compensation adaptive control for enhanced tracking: application to rmpkms. *Advanced Robotics*, Taylor & Francis, pp. 1-16, 2016.
- [4] M. Liu, C. LI, C. LI, "Dynamics analysis of the gough-stewart platform manipulator," *IEEE Transactions on Robotics and Automation*, v. 16, n. 1, p. 94-98, 2000. J. Clerk Maxwell, *A Treatise on Electricity and Magnetism*, vol. 2, Oxford: Clarendon, 1892, pp.68-73.
- [5] H. Guo, Y. Liu, G. Liu, and H. Li, "Cascade control of a hydraulically driven 6-DOF parallel robot manipulator based on a sliding mode". *Control Engineering Practice*, v. 16, n. 9, p. 1055-1068, 2008.
- [6] F.A. Lara-Molina, K.A. Takano, and E.H. Koroishi. "Set-Point Regulation of a Robot Manipulator with Flexible Joints Using Fuzzy Control." *2015 12th Latin American Robotics Symposium and 2015 3rd Brazilian Symposium on Robotics (LARS-SBR)*. IEEE, 2015.
- [7] M. Eftekhari, M. Eftekhari, and H. Karimpour. "Neuro-fuzzy adaptive control of a revolute stewart platform carrying payloads of unknown inertia." *Robotica* 33.09 (2015): 2001-2024.
- [8] Y. Huang, D. M. Pool, O. Stroosma, Q. P. Chu, and M. Mulder, "A Review of Control Schemes for Hydraulic Stewart Platform Flight Simulator Motion Systems," *AIAA Modeling and Simulation Technologies Conference*, California, pp. 1436-1450, January 2016
- [9] C. Gao, D. Cong, J. Han, Z. Yang and X. Wang, "Self-Calibration of a 6-DOF Redundantly Actuated Parallel Mechanism," *2016 IEEE International Conference on Mechatronics and Automation*, Japan, pp. 128-132, August 2016.
- [10] F. A. Lara-Molina, J.M. Rosário, D. Dumur and P. Wenger, "Robust generalized predictive control of the Orthoglide robot," *Industrial Robot: An International Journal*, 41(3), p. 275-285, 2014.
- [11] F.A. Lara-Molina, J.M Rosário and D. Dumur, "Robust generalized predictive control of Stewart-Gough platform," *Robotics Symposium, 2011 IEEE IX Latin American and IEEE Colombian Conference on Automatic Control and Industry Applications (LARC)*, p. 1-6, 2011.
- [12] B. Dasgupta, and T. S. Mruthyunjaya. "Closed-form dynamic equations of the general Stewart platform through the Newton-Euler approach." *Mechanism and machine theory* 33.7 (1998): 993-1012.